Electron correlation and dimerization in *trans*-polyacetylene: Many-body perturbation theory versus density-functional methods

Sándor Suhai
Molecular Biophysics Department, German Cancer Research Center, Im Neuenheimer Feld 280, D-69120 Heidelberg, Germany
(Received 27 January 1995)

Structural and energetic aspects of the Peierls-type lattice dimerization were investigated in infinite, one-dimensional, periodic *trans*-polyacetylene (*t*-PA) using many-body perturbation theory (MBPT) and density-functional theory (DFT). Cohesive properties and dimerization parameters were obtained first for the classical Coulomb potential in the Hartree approximation and then by gradually turning on exchange and correlation potentials. Besides the nonlocal Hartree-Fock exchange, several other exchange functionals were used incorporating gradient corrections as well. For MBPT, electron correlation was included up to the fourth order of the Møller-Plesset scheme and the behavior of lattice sums for different PT terms was analyzed in detail. The electrostatic part of the infinite lattice sums was computed by the multipole expansion technique. In solving the polymer Kohn-Sham equations, the performance of several different correlation potentials was studied again including different gradient corrections. Atomic basis sets of systematically increasing size, in the range of double-zeta to triple-zeta (TZ) up to TZ (3*df*,3*p*2*d*), were used in all calculations to construct the symmetry-adapted (Bloch-type) polymer wave functions, to fully optimize the structures, and to extrapolate different physical quantities to the limit of a hypothetical infinite basis set. Comparison of the different DFT results with MBPT and with experiments demonstrated the importance of gradient terms both for exchange and correlation. On the other hand, the best DFT functional, using a medium-size atomic basis set, excellently reproduced the cohesive and dimerization energies obtained for infinite *t*-PA at the MP4/TZ(3*d*2*f*,3*p*2*d*) level and provided dimerization parameters close to experiment. The experimentally observed lattice spacing of 2.46±0.01 Å will be correctly predicted both at the MBPT and DFT levels with 2.48 and 2.44 Å, respectively.

I. INTRODUCTION

Trans- polyacetylene (*t*-PA), the simplest organic polymer, still remains the prime model as a Peierls system with broken-symmetry ground state and as a testing ground for theories of electronic interactions in quasi-one-dimensional solids.[1–3] In crystalline form, PA can be doped to change its conductivity over many orders of magnitude[4] and it forms crystals of high enough quality to study its three-dimensional (3D) structure by x-ray,[5,6] neutron diffraction,[7] as well as by *nmr* spectroscopy.[8] The PA crystals consist of two dimerized chains per unit cell and have either the $P2_1/n$ (Ref. 4) or $P2_1/a$ (Ref. 6) space group. The experimentally found dimerization amplitude, which is the displacement of a C atom projected onto the polymer axis (Fig. 1), is $u_0=0.026$ Å.[5,6]

To identify the driving force behind this lattice dimerization, a large number of theoretical studies have been devoted to different aspects of this problem. According to the Peierls theorem,[9] which is rigorous for noninteracting fermions in a strictly 1D system, the equidistant nuclear configuration of solids with partially filled energy bands (metals) is unstable against nuclear distortions that enlarge the unit cell and introduce a forbidden gap into the single-particle energy spectrum at the new Brillouin-zone boundaries. The Peierls model couples phonons of wave vector $2k_{\mathrm{Fermi}}$, with band electrons at the Fermi surface thereby lowering the energy of the occupied levels and raising that of the unoccupied ones. For small distortions u, the electronic energy is proportional to $u^2\ln u$, while the elastic energy is quadratic in u, so that the system becomes unstable for an arbitrary small electron-phonon coupling. Though the argument of Peierls does not strictly apply for interacting fermions even at the Hartree-Fock (HF) level, investigations of the second variation of the HF total energy may point to instabilities that could be interpreted as precursors of a Peierls-type lattice dimerization.[10–12] The Peierls distortion is, furthermore, not a *transition* in a strict sense[13] since, within the framework of the Born-Oppenheimer approximation,

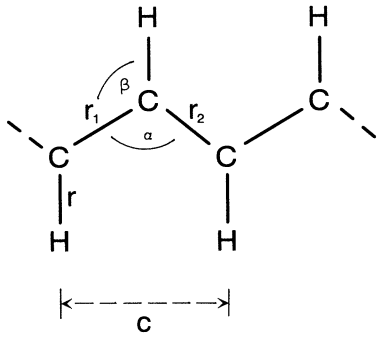

FIG. 1. The geometrical structure of the quasi-one-dimensional *trans*-polyacetylene (*t*-PA) chain also defining the conformational variables optimized in structure determinations. The polymer was always kept planar in these calculations.

the dynamical aspects of the dimerization process are not included. The HF instabilities may still provide an extremely useful hint on how to optimize the nuclear framework to reduce not only the HF, but also the exact total energy.

There is, on the other hand, considerable evidence of the importance of electron correlation effects both in finite polyenes and in *t*-PA itself and, therefore, the generalization of the Peierls theorem including electron-electron interactions has been of great recent interest.[1–3] The main goal of the present paper is to systematically study the role of different forces (electrostatic, exchange, and correlation) on the dimerization amplitude of *t*-PA starting from first principles and to compare the description of the corresponding exchange-correlation effects using different orders of many-body perturbation theory (MBPT), a well as various functionals in the framework of density-functional theory (DFT). Our investigations will focus on two aspects of the dimerization process in *t*-PA: (i) on the individual role of (classical) Coulomb, exchange, and correlation interactions in the structural and electronic properties of the infinite one-dimensional chain and (ii) on the possibility of describing electron correlation effects in those interactions by using different exchange-correlation potentials within the DFT approach. Besides experiments, it will also be of interest to compare the DFT results with different orders of MBPT for the same system. A number of atomic basis sets of systematically increasing size will be employed for both schemes to be able to extrapolate the computed quantities to the limit of a hypothetical infinite basis set.

From the previous DFT investigations of the *t*-PA lattice dimerization problem, Mintmire and White[14] found a dimerized ground state using the linear-combination-of-atomic-orbitals–local-density-functional (LCAO-LDF) approach with the Gaspar-Kohn-Sham potential. The fact that the bond alternation provided by this method is less than the experimental value by roughly a factor of 3 was traced back by these authors to their low value of 0.3 eV, obtained for the band gap. Similar results with a nonvanishing, but definitely too small bond alternation were obtained by Vogl and Campbell.[15,16] Ashkenazi *et al.*[17] employed the linearized-augmented-plane-wave method within the local-density approximation. Despite the use of highly converged basis sets and an estimated accuracy of the total energy of 0.07 millihartree (mhartree) per CH unit, they did not find an energy minimum for nonzero lattice distortion. Springborg *et al.*[18] utilized the linear-muffin-tin-orbital method and found Δr values in good agreement with experiments even though their gap values of about 0.6 eV were similar to those of Mintmire and White.[14] Paloheimo and von Boehm[19,20] used the self-consistent linear-combination-of-Gaussian-orbitals method with the exchange-correlation (XC) potential of Ceperley and Alder parametrized by Perdew and Zunger[21] and obtained $u_0=0.01$ Å with $\Delta E=7$ meV, in agreement with the results of Mintmire and White.[14] Interestingly, Paloheimo and von Boehm did not get dimerization at the Hartree level, but this may be a consequence of the fact that they did not perform a complete geometry optimization far away from the neighborhood of the experimental bond lengths, where the Hartree lattice becomes Peierls instable (see below). They observed, on the other hand, the important fact that the most essential contributions for lowering the energy of the dimerized *t*-PA come from the π-electron system. For MBPT, the influence of electron correlation on the dimerization of *t*-PA was investigated by the present author,[22–24] using the Møller-Plesset partitioning scheme at second order. The HF dimerization amplitude of $u_0=0.046$ Å was shown to be reduced by correlation effects of 0.037 Å. Similar results were obtained by König and Stollhoff,[25] using a local ansatz for the wave function and linearized coupled cluster equations to compute the correlation contributions.

The present paper will be organized as follows: Section II gives brief review of the methodological aspects of the computation of the ground-state correlation energy in infinite polymers, using the MBPT and the LCAO-DFT approach. Section III presents the structural and energetic properties of the equidistant and dimerized *t*-PA obtained in the Hartree approximation. Section IV treats exchange effects within the HF and DFT schemes, while Section V introduces electron correlation. Finally, Sec. VI discusses the results and summarizes the conclusions.

II. ELECTRON CORRELATION IN EXTENDED SYSTEMS: PERTURBATION THEORY VS DENSITY-FUNCTIONAL METHODS

The method of calculating electron correlation effects for infinite systems using different orders of MBPT has been described in more detail earlier with several applications to semiconducting and metallic polymers.[22–24,26–30] Here, we only provide a concise summary of the basic expressions to be able to define the various theoretical levels as applied to *t*-PA. The computational procedure is a generalization of the methods worked out by Pople and co-workers over the past decades for molecules,[31–37] to the case of infinite crystals using additional symmetry operations (translation and helical rotation) and different numerical procedures of solid-state theory. The computer programs developed in our laboratory for electronic structure calculations on crystals also make intensive use of several techniques and modules of the Gaussian molecular packages up to Gaussian 92/DFT.[34]

After a number of successful applications in solid-state physics,[38–42] computational methods based on DFT are developing to an economical, general tool in molecular[43–45] and polymer physics[29,30,46–50] as well. Among the first calculations along these lines, Mintmire and White used an $X\alpha$ scheme and Gaussian basis orbitals,[46,47] von Boehm, Kuivalainen, and Calais[48] solved the Kohn-Sham equations by applying the Perdew-Zunger exchange-correlation functional, while Springborn and Anderson[49] applied linearized muffin-tin orbitals to the same problem and te Velde and Baerends[50] developed a general program system to treat periodic systems of any dimension within the LCAO-DFT approach. The traditional method of accurately calculating the electronic properties of polymer crystals from first principles *(ab initio* in the quantum chemical sense) is to first perform a

HF calculation[51,52] followed by a subsequent computation of electron correlation effects using different orders of MBPT.[22,28,30] In the case of a careful Coulomb integral handling and using proper numerical schemes in performing the infinite lattice sums,[53] the first step scales essentially as $O(\nu^2-\nu^{2.5})$ for a polymer, where ν is the number of atomic basis functions in the (translationally invariant) unit cell.

The computational expense of MBPT procedures, on the other hand, starts formally with $O(\nu^5)$ in second order and increases rapidly for higher orders. Though the systematic use of localized Wannier orbitals and of advanced integral transformation and selection procedures within the Møller-Plesset (MP) PT scheme[53] reduces this burden and makes it possible to perform geometry optimizations and vibrational frequency calculations for polymers with medium size unit cells (6–8 atoms) up to the MP4 level, even using extended atomic basis sets (e.g., several d and f functions on first row atoms),[29,30] such calculations are clearly too demanding to become a routine in polymer theory. For the investigation of physical and chemical properties that do not explicitly depend on the wave function itself, DFT may provide an alternative way of estimating the correlation effects at a relatively modest cost, formally $O(\nu^3)$, which may be reduced by an efficient implementation.[37] Therefore, DFT polymer studies including electron correlation will scale again as only $O(\nu^2-\nu^{2.5})$, similar to the HF case. Since, furthermore, a number of refined exchange-correlation potentials have been designed in the past years, most of them containing gradient corrections to include the effect of local fluctuations in the electron density, the quality of DFT methods in relation to polymeric systems deserves reconsideration and careful comparison both with experimentally observable quantities and with the results of high-quality correlated (MP2-MP4) calculations, using the same atomic basis sets.

In order to construct the zeroth-order wave function, $\Phi_0 \equiv \Phi_{\rm HF}$, we first have to solve the crystal HF problem. In the case of the spin-restricted theory the corresponding Fock operator consists of kinetic energy, nuclear attraction, Coulomb and exchange terms in the form

$$\begin{aligned}\hat{F}^{\rm HF}(\mathbf{r}_l) &= \hat{T}+\hat{V}+\hat{J}+\hat{K} \\ &= -\tfrac{1}{2}\Delta_{\mathbf{r}_l} - \sum_{h=-N_c/2}^{+N_c/2}\sum_{A=1}^{n_A}\frac{Z_A}{|\mathbf{r}_l-\mathbf{R}_h-\mathbf{R}_A|} \\ &\quad + \int d^3\mathbf{r}_m \frac{\rho(\mathbf{r}_l,\mathbf{r}_l)}{|\mathbf{r}_l-\mathbf{r}_m|} \\ &\quad - \int d^3\mathbf{r}_m \frac{\rho(\mathbf{r}_l,\mathbf{r}_m)}{|\mathbf{r}_l-\mathbf{r}_m|}\hat{P}(\mathbf{r}_l,\mathbf{r}_m)\ , \end{aligned} \tag{1}$$

where N_c+1 is the number of elementary cells, n_A is the number of atoms per cell, and Z_A is the core charge of the atom A at position $\mathbf{R}_A$. The first-order density matrix, $\rho(\mathbf{r}_l,\mathbf{r}_m)$, will be constructed from the (doubly) occupied Bloch spinorbitals by numerical integration over the first Brillouin zone (BZ) and the Bloch orbitals $\phi_n^{\mathbf{k}}(\mathbf{r}_1)$ will be obtained as self-consistent solutions of the Hartree-Fock equations of the crystal.[51,52] In the MP partitioning scheme[54] of MBPT, the many-electron Hamiltonian $\hat{\mathcal{H}}$ will be taken as the Fock Hamiltonian plus a perturbation:

$$\hat{\mathcal{H}}=\hat{\mathcal{H}}_0+\hat{\mathcal{V}}=\sum_l \hat{F}^{\rm HF}(\mathbf{r}_l)+\left\{\hat{\mathcal{H}}-\sum_l \hat{F}^{\rm HF}(\mathbf{r}_l)\right\}\ . \tag{2}$$

The solution of the polymer HF equations,

$$\hat{F}^{\rm HF}(\mathbf{r}_l)\phi_n^{\mathbf{k}}(\mathbf{r}_l)=\varepsilon_n^{\mathbf{k}}\phi_n^{\mathbf{k}}(\mathbf{r}_l)\ , \tag{3}$$

provides a set of one-electron Bloch functions, $\phi_n^{\mathbf{k}}(\mathbf{r}_l)$, with quasimomentum $\mathbf{k}$ in band n that will be expressed as linear combinations of symmetry adapted basis orbitals in the form

$$\phi_n^{\mathbf{k}}(\mathbf{r})=\sum_{a=1}^{\nu} c_{an}^{\mathbf{k}}\psi_a^{\mathbf{k}}(\mathbf{r})\ , \tag{4}$$

where ν is the number of basis orbitals, $\psi_a^{\mathbf{k}}(\mathbf{r})$, per elementary cell of the crystal taken as a Bloch-type linear combination of contracted Gaussian-type atomic orbitals (CGTO's):

$$\psi_a^{\mathbf{k}}(\mathbf{r})=(N_c+1)^{-1/2}\sum_{h=-N_c/2}^{+N_c/2}\exp\{i\mathbf{k}\cdot\mathbf{R}_h\}\chi_a^h(\mathbf{r})\ . \tag{5}$$

The CGTO $\chi_a^h(\mathbf{r})=\chi_a(\mathbf{r}-\mathbf{R}_a-\mathbf{R}_h)$ will be centered in the cell h at $\mathbf{R}_a+\mathbf{R}_h$. The number of atomic basis functions per CH unit is a crucial parameter at all theoretical levels and it will be investigated in detail in the subsequent sections. The zeroth-order N-electron wave function of the crystal, $\Phi_{\rm HF}$, will be written as a Slater determinant built from the doubly filled Bloch functions,

$$\begin{aligned}\Phi_{\rm HF}&=(N!)^{-1/2} \\ &\quad\times\det[\ldots\phi_n^{\mathbf{k}}(\mathbf{r}_i)\alpha(\sigma_i)\phi_n^{\mathbf{k}}(\mathbf{r}_{i+1})\beta(\sigma_{i+1})\ldots]\ .\end{aligned} \tag{6}$$

The HF energy of the crystal will then be obtained as the sum of the zeroth- and first-order terms of PT,

$$E_{\rm HF}=\mathcal{E}^{(0)}+\mathcal{E}^{(1)}=\sum_{(\mathbf{k},n)}^{\rm (occ)}\varepsilon_n^{\mathbf{k}}+\langle\Phi_{\rm HF}|\hat{\mathcal{V}}|\Phi_{\rm HF}\rangle\ , \tag{7}$$

while in higher orders we get correlation corrections to it: $E_{\rm corr}=\mathcal{E}^{(2)}+\mathcal{E}^{(3)}+\mathcal{E}^{(4)}$. The second- and third-order terms were previously analyzed for different polymers including *t*-PA.[22,28] Of special interest will be the analysis of different contributions in fourth order, originating from single (S), double (D), triple (T), and quadruple (Q) excitations:[33]

$$\mathcal{E}^{(4)}=\mathcal{E}_S^{(4)}+\mathcal{E}_D^{(4)}+\mathcal{E}_T^{(4)}+\mathcal{E}_Q^{(4)}\ , \tag{8}$$

where $\mathcal{E}_Q^{(4)}$ includes the so-called renormalization term,[32] with double excitations that partially cancel quadruple terms. All four contributions in Eq. (8) are individually size consistent. In presenting our results, it will be reasonable to combine the fourth-order contributions from double and quadrupole substitutions as $\mathcal{E}_{\rm DQ}^{(4)}$, since $\mathcal{E}_{\rm D}^{(4)}$ and $\mathcal{E}_Q^{(4)}$ both contain large terms from unlinked clusters that partly cancel each other.[32] The detailed

form of the above MBPT terms for infinite systems was published earlier for second,[22] third,[28] and fourth[29] orders, respectively.

In their local-spin-density (LSD) form, DFT methods simply replace the HF exchange functional with an XC functional of the local electron-spin densities ρ_α and ρ_β.[39–43] Gradient corrected methods (frequently referred to as nonlocal functionals) also include the spin-density gradients ∇_{ρ_α} and ∇_{ρ_α}, to account for local fluctuations in the electron density. The Hohenberg-Kohn theorem[38] ensures that there exists a unique functional which exactly determines the ground-state energy. Since the exact form of the functional is unknown, several approximate forms of the XC potential have been proposed.[21,55–63] In the most widely used formulation of DFT, the Kohn-Sham (KS) theory,[39] an LCAO-type basis set expansion of one-electron orbitals is obtained via a self-consistent procedure analogous to that of the conventional HF theory. This allows correlation to be included at the SCF level at some extra cost. An alternative to computing the KS density is to obtain the electron density via the one-electron orbitals resulting from a HF calculation and substituting it into the LSD expression. This hybrid method involves performing a single numerical integration after solving the HF problem and may be even more cost effective than the KS procedure.

For the DFT formulation of the polymer electronic structure problem, the Fock operator will be taken in the form analogous to Eq. (1), with the difference that the HF exchange will be substituted with the appropriate exchange-correlation term:

$$\hat{F}^{\mathrm{DFT}}=\hat{T}+\hat{V}+\hat{J}+\hat{F}_{\mathrm{XC}} , \tag{9}$$

and the crystal HF equations will go over to the corresponding Kohn-Sham equations.[39] The self-consistent and gradient procedures for solids are again in complete analogy to the molecular case and the appropriate modules of the G92/DFT program package[34] have been utilized, after extension for translational and helical symmetry operations, for their solution. Several computational aspects of this procedure specific to infinite systems (handling of infinite lattice sums, numerical accuracy of BZ manipulations, etc.) will be reported elsewhere.[64]

The functionals used in our computations consist of separate exchange and correlation parts, respectively. For the exchange part, we used the free-electron gas functional proposed by Slater (S),[55] the gradient-corrected functional designed by Becke (B) (Ref. 60) to correctly reproduce the exact asymptotic behavior of the exchange energy density for a finite many-electron system, and the mixture of the exact HF exchange with the Slater functional, the BHH procedure.[63] The correlation part was either ignored (leading to the HFS, HFB, and BHH theories) or it was treated by the local spin-density theory as parametrized by Vosko, Wilk, and Nusair (VWN),[57] by the gradient-corrected functional of Lee, Yang, and Parr (LYP),[61] as transformed by Mielich *et al.*,[62] and by the functional of Perdew and Wang (P86).[59] While the VWN functional reproduces exact uniform electron-gas results, the LYP functional was designed (initially by Colle and Salvetti[56]) to calculate the exact nonrelativistic energy of the He atom from the HF density. The correlation functionals can be combined with exchange terms providing different computational schemes: S-VWN, S-LYP, B-VWN, B-P86, B-LYP, BHH-LYP. It also seemed worthwhile to test the combination of the exact HF exchange with the gradient-corrected LYP potential, the HF-LYP scheme. In the subsequent sections, we will report results obtained by the comparative application of these XC functionals to t-PA.

III. CLASSICAL COULOMB EFFECTS: THE HARTREE SCHEME

To understand the role of exchange and correlation effects in the structural and electronic properties of t-PA, the first question to ask is as follows: What is the ground state of the quasi-one-dimensional t-PA chain in the presence of a pure (classical) Coulomb potential when we first neglect any exchange or correlation interactions? The answer to this question will be given by the solution of the corresponding crystal Hartree equations:

$$\hat{F}^{H}(\mathbf{r}_l)\phi_n^{\mathbf{k}}(\mathbf{r}_l)=\varepsilon_n^{\mathbf{k}}\phi_n^{\mathbf{k}}(\mathbf{r}_l) ,$$
$$\hat{F}^{H}=\hat{T}+\hat{V}+\hat{J} . \tag{10}$$

The Hartree-type Bloch functions of Eq. (10), $\phi_n^{\mathbf{k}}(\mathbf{r}_l)$, will be expanded again in terms of CGTO's in the same manner as discussed for the HF case and defined by Eqs. (4) and (5), respectively. As a first step, we employed a

TABLE I. List of the applied sets of uncontracted Gaussian-type atomic basis functions, respectively.

Symbol of basis set	Uncontracted basis Components	N^a	Contracted basis Components	N^a	References[b]
DZ	$(9s5p/4s)$	28	$[4s2p/2s]$	12	65
DZ(d,p)	$(9s5p1d/4s1p)$	37	$[4s2p1d/2s1p]$	21	65,66
DZ(2d,2p)	$(9s5p2d/4s2p)$	46	$[4s2p2d/2s2p]$	30	65,66
TZ(2df,p)	$(11s6p2d1f/6s1p)$	55	$[5s3p2d1f/4s1p]$	38	66,67
TZ(3d2f,2pd)	$(11s6p3d2f/6s2pd)$	73	$[5s3p3d2f/4s2pd]$	58	66,67

[a]The total number of uncontracted or contracted atomic basis functions, respectively, resulting in the given basis set for the CH unit of t-PA.

[b]The first reference refers to the isotropic part of the basis set, the second one to the polarization functions used.

double-zeta-(DZ-) type atomic basis set[65] consisting of nine *s*- and five *p*-type atomic orbitals on carbon and of four *s* orbitals on hydrogen contracted according to the scheme shown in Table I.

To find the ground-state configuration of the Hartree solution, we optimized the geometry of *t*-PA, shown in Fig. 1, in two steps. First, we constrained the bond lengths r_1 and r_2 to be equal (equidistant chain) and optimized the remaining conformational variables keeping the polymer planar. The resulting Hartree total energy, E_H (equ), per CH units is depicted in Fig. 2, as a function of r_1 ($=r_2$). It is interesting to note that even though the polymer is stable in the Hartree approximation, with a cohesion energy of -0.232002 hartree (-6.313 eV) per CH unit at the DZ level, the C-C bonds of the optimized equidistant structure ($r_0=1.8887$ Å) are unusually large. A subsequent relaxation of the constraint $r_1=r_2$ leads to an optimized bond alternating Hartree structure with $r_1=1.8428$ Å and $r_2=1.9344$ Å, respectively, at this basis set level. As we can see from Fig. 2, the bond alternation [$\Delta r(H)=0.0916$ Å] significantly further stabilizes the polymer, by -0.21 mhartree (-0.0057 eV) per CH unit. Figure 3 shows the optimized values of r_2 (and the resulting Δr) for fixed values of r_1 (all other variables being optimized as well). This nearly linear r_2 vs r_1 relationship is a general feature of the dimerization of *t*-PA and it will also be observed at higher theoretical levels. The E_H vs Δr relationship shown in Fig. 4 reveals, on the other hand, that the potential-energy surface of the dimerization process is very flat at the Hartree level and the corresponding force constants are by an order of magnitude smaller than those obtained after turning on exchange and correlation effects (to be discussed in the next sections). This trend is similar to the dependence of the stabilization energy of the bond alternation, ΔE, as a function of Δr shown by Fig. 5: In the region of physically relevant values of Δr, the corresponding Hartree values of ΔE are approximately an order of magnitude smaller than those obtained by including exchange and/or correlation effects, respectively.

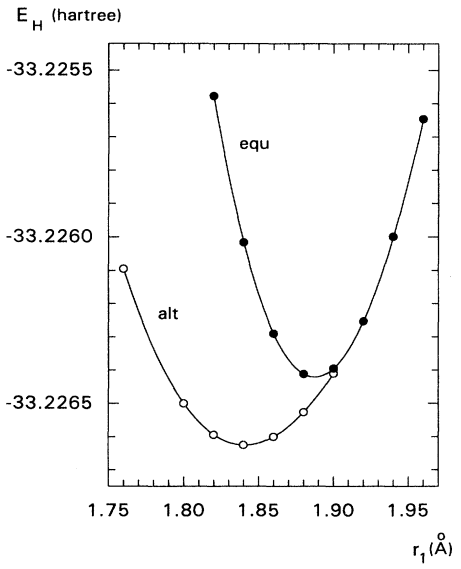

FIG. 2. The Hartree energy per CH unit of equidistant (equ) and bond-alternating (alt) *t*-PA, as a function of the bond length r_1. For the equidistant chain, the constraint $r_1=r_2$ has been applied, while optimizing all other conformational variables. This constraint was lifted during optimization of the bond-alternating structure.

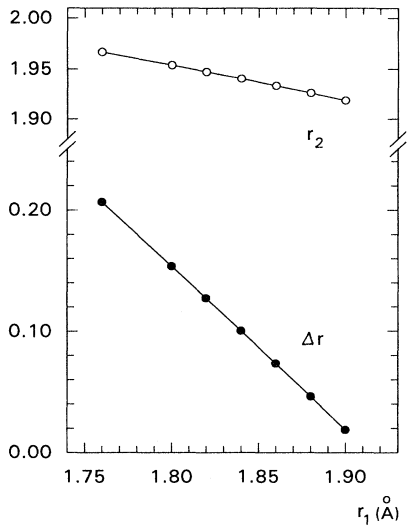

FIG. 3. r_2 and $\Delta r=r_2-r_1$ as a function of r_1 (defined in Fig. 1) in the case of bond-alternating *t*-PA, obtained in the Hartree approximation, using the DZ basis set.

Since the Hartree energy differences between equidistant and dimerized *t*-PA chains are rather small, it is necessary to prove that the above results are independent of basis set artifacts. For this purpose, the lattice optimization has been repeated by systematically increasing the number of CGTO's applied in Eq. (10). Table I defines

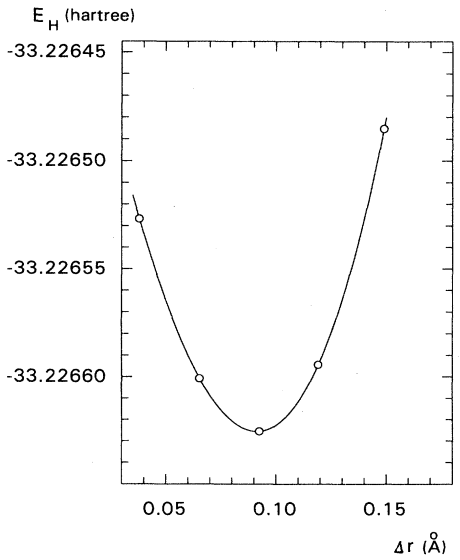

FIG. 4. The Hartree energy, E_H, per CH unit of *t*-PA as a function of the bond alternation, Δr (DZ basis set).

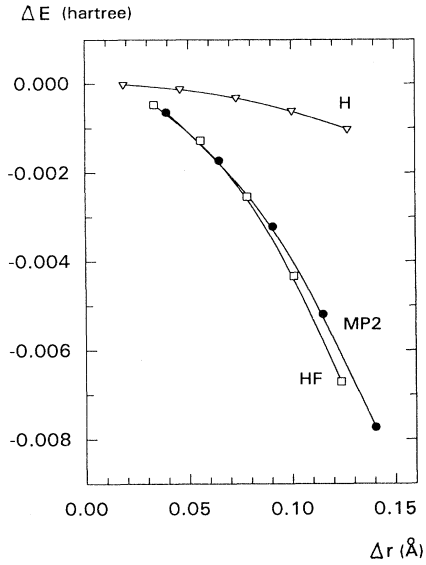

FIG. 5. The stabilization energy per CH unit, due to bond alternation in t-PA, $\Delta E = E_{\text{tot}}(\text{alt}) - E_{\text{tot}}(\text{equ})$, obtained as a function of Δr, by using different methods at the DZ basis set level.

the atomic basis sets that were used in these studies. The isotropic part of the basis sets refers to orbitals occupied in the ground state of the corresponding atoms. The exponents and contraction coefficients of these orbitals have been taken from the double-zeta (DZ) and triple-zeta (TZ) schemes of Dunning.[65,66] The exponents of the polarization functions used to complement the isotropic part originate partly from the library of the Gaussian program packages[34] and partly from the correlation optimized sets of Dunning.[67] As shown by Fig. 6 in the case of the cohesion energy, E_{coh}, the Hartree values turn out to be relatively independent of the number of CGTO's. The same trend was observed for ΔE as well. We may conclude, therefore, that electron-electron interactions lead, even in the simple Hartree approximation, to a bond-alternating lattice for t-PA though the extra binding energy, due to the dimerization is relatively small at this level.

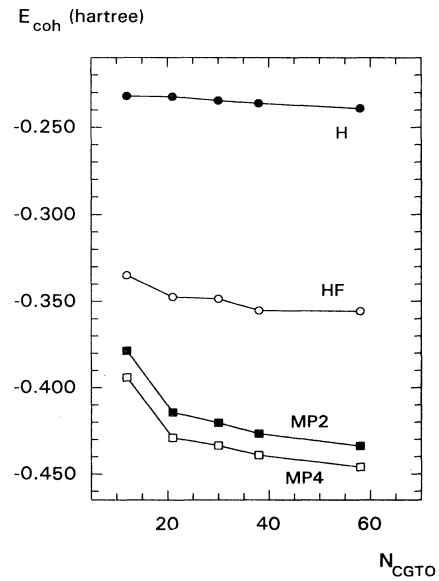

FIG. 6. The cohesion energy per CH unit in equidistant t-PA, obtained as a function of the number of CGTO's at different theoretical levels.

IV. EXCHANGE EFFECTS: THE HF AND DFT SCHEMES

The inclusion of the (exact) exchange part of the Fock operator in Eq. (1) influences the physical properties of t-PA in several ways. Some aspects of the energetic and structural properties of different PA polymers were discussed in detail at the HF level in a recent paper,[27] where references to earlier publications were also given. Here, we only briefly mention those aspects of the HF description, at the DZ basis set level first, which will be relevant for comparison with the new DFT and MBPT results, respectively. At first, as expected, the appearance of the exchange operator $\hat{K}$ in Eq. (1) substantially decreases the cohesion energy of the lattice (Fig. 6) by about -105 mhartree (-2.86 eV) per CH unit (50%), in comparison with the corresponding Hartree value. Furthermore, as compared with the Hartree lattice, the C-C bond lengths of equidistant t-PA will be reduced, due to exchange, by nearly 0.5 Å to $r_0 = 1.3962$ Å at the DZ basis set level (Fig. 7). Atomic polarization functions of the d and f type are also more important in calculating the matrix elements of $\hat{K}$ than they were for $\hat{J}$. Their effect amounts to about -40 mhartree (-1.09 eV) decrease per CH unit

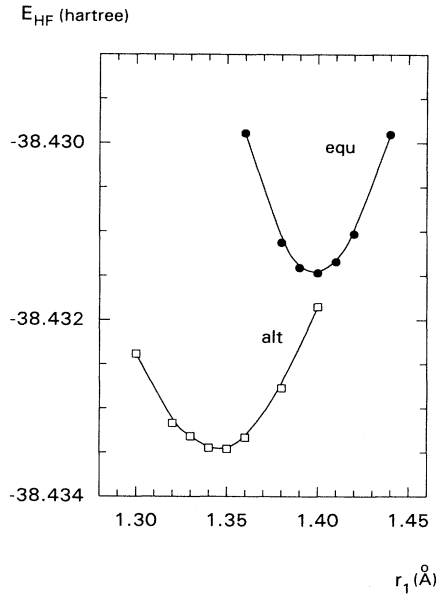

FIG. 7. The HF energy, E_{HF}, per CH unit of equidistant (equ) and bond-alternating (alt) t-PA, as a function of the bond length r_1. For the equidistant chain, the constraint $r_1 = r_2$ has been applied, while optimizing all other conformational variables. This constraint was lifted during optimization of the bond-alternating structure.

in E_{coh}, at the HF level. The optimization of the lattice, in the same manner as described above for the Hartree method, results in the energetic picture shown in Fig. 7. Due to E_x, the extra stabilization energy of the dimerized lattice, as compared with the optimized equidistant chain, decreases by -2.017 mhartree (-0.055 eV) per CH unit at the DZ level. The relationship of the HF dimerization parameters r_1, r_2, and Δr (Fig. 8) is similar to the Hartree case, though $\partial(\Delta r)/\partial r_1$ will be somewhat reduced, due to $\hat{K}$. Furthermore, a comparison of Figs. 2 and 7 also reveals that the phonon frequencies of *t*-PA will sensitively depend on the proper inclusion of exchange effects. (The detailed study of the corresponding vibrational spectra of PA, including correlation effects as well, will be the subject of a forthcoming paper).

From the dependence of the HF total energy on Δr (Fig. 9), we can infer that the energetically optimal value of Δr (HF) increased by 0.0158 Å from the corresponding Hartree value (Fig. 4). To get a better insight into the mechanism of the lattice dimerization in *t*-PA, it is instructive to gradually turn on the contribution of the operator $\hat{K}$ in Eq. (1) and study its effect on the bond alternation. The corresponding results, depicted in Fig. 10, exhibit a nearly linear relationship between Δr and E_x. The gradual increase of Δr is, of course, a small geometrical change resulting from the superposition of two larger opposite effects, namely, the overall shortening of the C-C bonds, due to exchange (from nearly 1.9 to 1.4 Å on the average) and the parallel increase of the bond alternation. Finally, the basis set dependence of r_0 (HF) for the equidistant chain and of Δr (HF) for the dimerized chain are depicted in Figs. 11 and 12, respectively, showing that while r_0 (HF) is somewhat more sensitive to N_{CGTO}, Δr (HF) will be nearly saturated at the DZ (d,p) level. Extrapolations of the corresponding results to an infinite basis set provide the values of r_0 (HF) = 1.3833 Å and Δr (HF) = 0.1196 Å at the HF limit. The dependence on N_{CGTO} of the lattice stabilization energy, due to bond alternation (HF curve in Fig. 13), will be increased by about 20% in going from DZ to TZ ($3d2f,2pd$) and it converges to the HF limit of -2.462 mhartree (-0.067 eV).

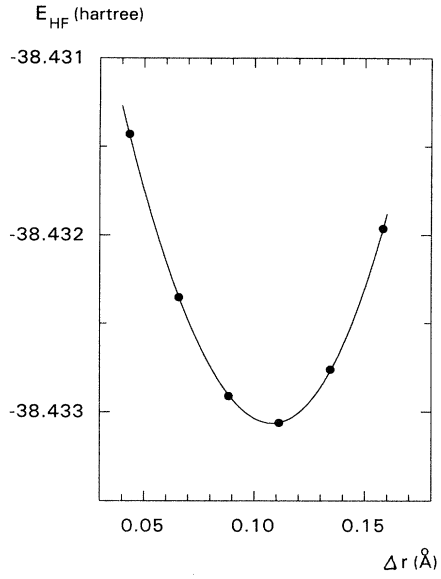

FIG. 9. The HF energy, E_{HF}, per CH unit of *t*-PA, as a function of the bond alternation, Δr (DZ basis set).

Turning now to the investigation of the performance of the *exchange-only* DFT formalism, we will first compare the above discussed quantities with their pendants obtained using the DZ basis set and the local (HFS) and gradient corrected (HFB, BHH) exchange functionals, re-

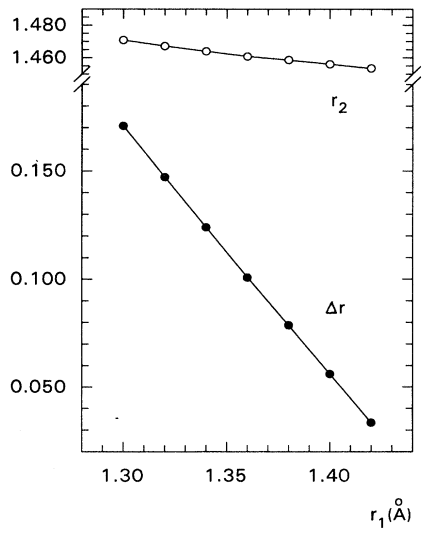

FIG. 8. r_2 and $\Delta r = r_2 - r_1$ as functions of r_1 (defined in Fig. 1), in the case of bond-alternating *t*-PA, obtained in the HF approximation using the DZ basis set.

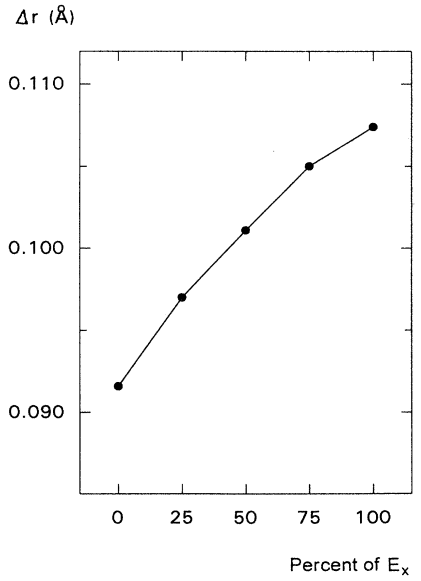

FIG. 10. The bond alternation, Δr, as a function of the exchange turned on stepwise in the Fock operator of *t*-PA.

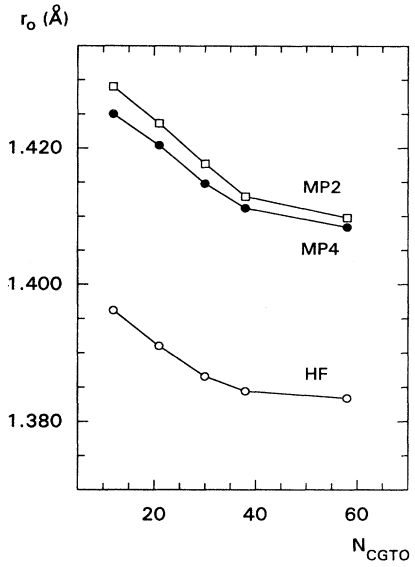

FIG. 11. The optimal C-C bond length, r_0, in equidistant t-PA, as a function of the number of CGTO's at different theoretical levels.

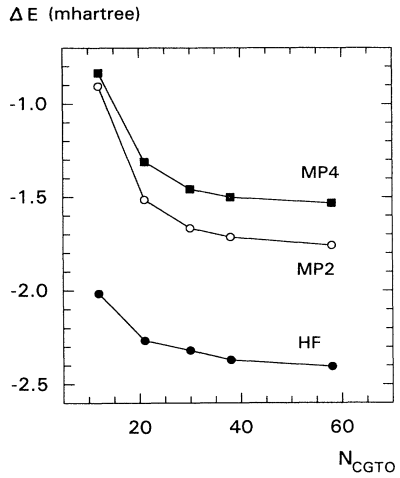

FIG. 13. The difference in the total energy per CH unit of bond-alternating and equidistant t-PA, as a function of number of CGTO's at different theoretical levels.

spectively, mentioned in Sec. II. Table II summarizes the corresponding results. We can see that the use of the Slater exchange strongly underestimates the bond alternation effect, both from the energetic and structural points of view, respectively, as compared with the exact exchange (or with experiment). The gradient correction in the Becke exchange improves somewhat upon the situation and, finally, the mixing of the Becke exchange with the Slater functional (BHH method[63]) leads to quite reasonable values both for u_0 and ΔE, respectively. The cohesion energy will be severely overestimated by the HFS method (-0.430 hartree) but very reasonably corrected by the gradient term in HFB (-0.355 hartree) and by the BHH procedure (-0.343 hartree) to reproduce the value of -0.335 hartree per CH unit obtained for the exact exchange.

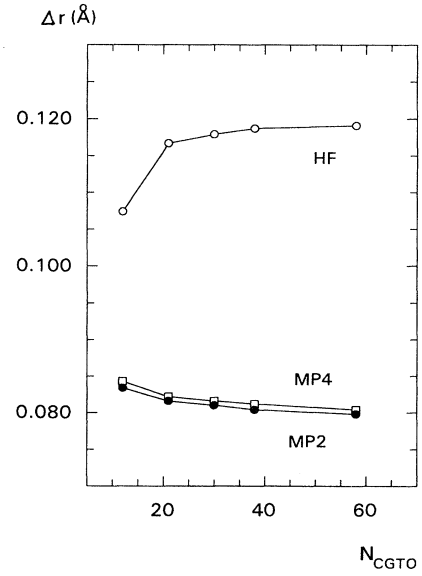

FIG. 12. The optimized bond alternation, Δr, in t-PA, as a function of number of CGTO's at different theoretical levels.

In view of these first DZ results, we selected the BHH functional to further study the role of the extension of the atomic basis set in the description of the dimerization process at the E_x (DFT) level. As demonstrated by Figs. 14 and 15, two sets of carbon d- and hydrogen p functions and at least one set of carbon f functions seem to be needed to stabilize r_0 and Δr for the (physically significant) second decimal digit. A similar conclusion can be drawn for the energetic aspects: the cohesion energy further decreases by about -18 mhartree, due to additional polarization functions (Fig. 16), while the dimerization energy, ΔE (BHH) (Fig. 17), decreases from -0.87 to -1.13 mhartree. The values of these quantities, extrapolated for an infinite basis set, are collected in Table III to facilitate the comparison of the different methods.

V. CORRELATION EFFECTS: PERTURBATION THEORY VS DFT

Looking first at the qualitative structural effects of electron correlation at the DZ level of second order MBPT (MP2), we may observe (comparing Fig. 18 with Fig. 7) that E_c substantially expands the equidistant t-PA lattice. This effect amounts to about 0.025-0.030 Å and it is nearly independent of the atomic basis sets applied (cf. Fig. 11). The bond-alternating structure is again more stable than the equidistant one (Fig. 18), but the energy difference will be reduced from -2.02 mhartree (HF) to -0.91 mhartree (MP2) at the DZ level. Furthermore, r_2 and Δr show the same linear dependence on r_1 as observed previously for the HF method (Fig. 19). The com-

TABLE II. Energetic and structural parameters of *t*-PA calculated at different theoretical levels, as discussed in the text (DZ basis set). The total energy of the equidistant chain, E(equ), the cohesion energy, E_{coh}(equ), and the energy difference between the alternating and equidistant chains, ΔE, are given in hartree per CH unit, while the optimal C-C distance in the equidistant chain, r_0, the bond alternation, Δr, and the lattice dimerization amplitude, u_0, are given in Å.

Potential	E(equ)	r_0	E_{coh}(equ)	ΔE(alt-equ)	Δr	u_0^a
H	−33.226 422	1.8887	−0.232 002	−0.000 210	0.0916	0.0259
HF	−38.431 473	1.3962	−0.334 900	−0.002 017	0.1074	0.0304
HFS	−37.895 804	1.4189	−0.430 406	−0.000 133	0.0182	0.0051
HFB	−38.449 897	1.4392	−0.355 441	−0.000 167	0.0476	0.0135
BHH	−38.438 898	1.4042	−0.343 644	−0.000 872	0.0819	0.0232
SVWN	−38.476 187	1.3994	−0.481 434	−0.000 071	0.0158	0.0045
SLYP	−38.127 032	1.3991	−0.487 494	−0.000 226	0.0055	0.0015
BVWN	−39.030 615	1.4183	−0.404 412	−0.000 230	0.0223	0.0063
BP86	−38.698 375	1.4163	−0.429 384	−0.000 175	0.0187	0.0053
BLYP	−38.679 314	1.4189	−0.410 778	−0.000 416	0.0120	0.0034
BHHLYP	−38.669 905	1.3864	−0.400 489	−0.000 932	0.0741	0.0210
HFLYP	−38.664 368	1.3711	−0.393 635	−0.000 891	0.1009	0.0285
MP2	−38.529 520	1.4250	−0.378 641	−0.000 906	0.0834	0.0236
MP4	−38.583 102	1.4290	−0.417 174	−0.000 836	0.0843	0.0238

[a]Experimental value is $u_0 = 0.026$ Å (Ref. 6).

parison of the functional dependence of the MP2 total energy per CH unit on Δr (Fig. 20) with the corresponding HF results (Fig. 9) demonstrates that the correlation reduces the bond alternation. In the case of MP2 and MP4, this effect only weakly depends on N_{CGTO} (Fig. 12) and amounts to about 50%, leading from the HF limit of Δr(HF) = 0.1196 Å to 0.0786 and 0.0794 Å at the MP2 and MP4 levels, respectively. These latter values of Δr correspond to a dimerization amplitude of $u_0 = 0.024$ Å and they are in excellent agreement with the experimental value of 0.026 Å.[5,6] The alternating single and double bond lengths at the MP4 level are 1.4428 and 1.3634 Å, respectively, providing a lattice constant of $c = 2.48$ Å for *t*-PA, close to the experimental value of 2.46±0.01Å.[5] The extra binding energy associated with Δr will be reduced by about 30–35% due to correlation (Fig. 13). The gradual switching on of the E_c potential at the MP2 level (Fig. 21) reveals that Δr linearly depends on the

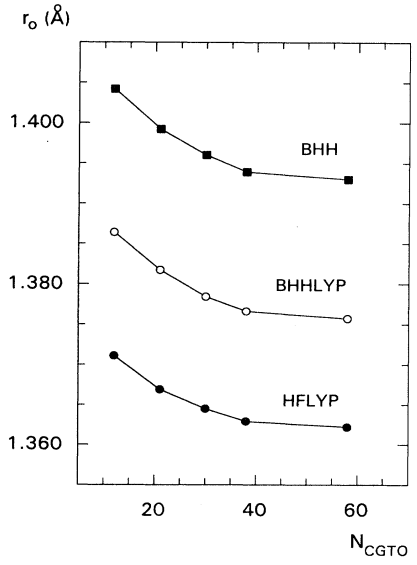

FIG. 14. The optimal C-C bond length, r_0, in equidistant *t*-PA, as a function of the number of CGTO's for different DFT potentials.

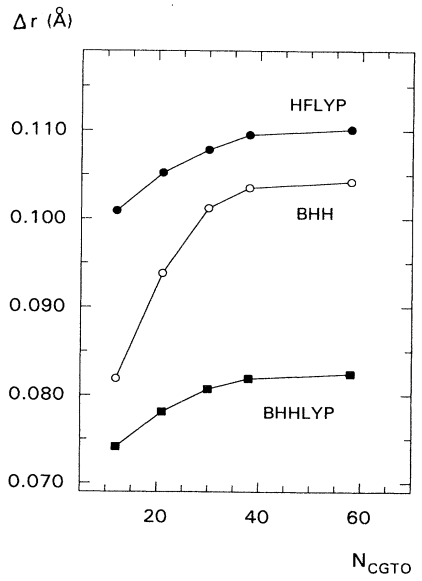

FIG. 15. The optimized bond alternation, Δr, in *t*-PA, as a function of the number of CGTO's for different DFT potentials.

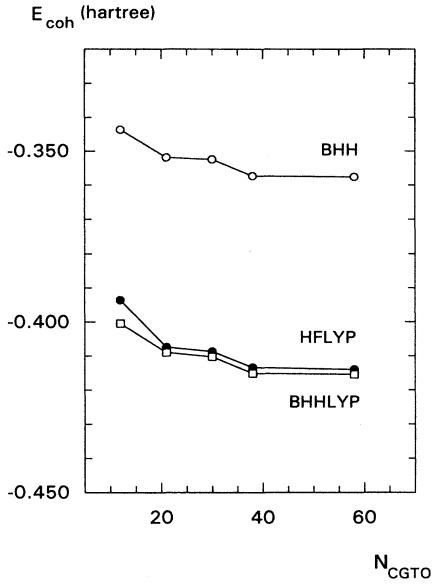

FIG. 16. The cohesion energy per CH unit in equidistant *t*-PA, obtained as a function of number of CGTO's for different DFT potentials.

amount of correlation included in the calculation, similarly to the exchange effect studied above.

The absolute values of the correlation energy, E_c, exhibit the expected strong dependence on the size of the atomic basis set both for MP2 and MP4, respectively (Fig. 22). They will be more than doubled in going from DZ to TZ($3d2f,2pd$) and extrapolations for $N_{\mathrm{CGTO}} \rightarrow \infty$ lead to the values of E_c(MP2) $= -209.2$ mhartee (-5.69 eV) and E_c (MP4) $= -243.1$ mhartree (-6.62 eV) per CH unit, respectively. E_c also substantially contributes to the cohesion energy of the *t*-PA lattice with -81.1 mhartree (-2.21 eV) per CH unit at the MP2 level and with -90.8 mhartree (-2.47 eV) at MP4, which is quite

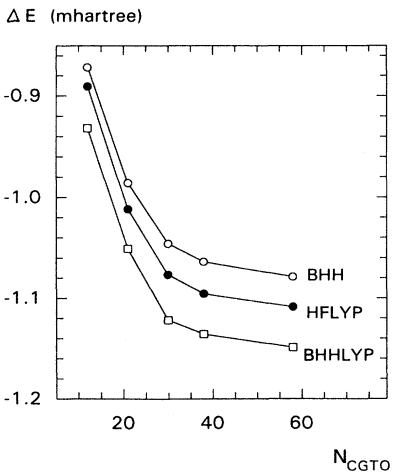

FIG. 17. The difference in the total energy per CH unit of bond-alternating and equidistant *t*-PA, as a function of number of CGTO's for different DFT potentials.

comparable to the binding energy due to exchange -119.9 mhartree (-3.26 eV) from Table III. The dependence of $\mathcal{E}^2$ on the intercellular interactions was reported earlier.[22] Interestingly, the lattice sum contribution to E_c in the third and fourth orders of PT turns out to be rather small. This effect can be traced back to the complex dependence of different PT terms, as functions of the number of interacting units taken into account in performing the lattice sums. Figure 23 provides an example for this effect in the case of alternating *t*-PA, using the TZ($3d2f,2pd$) basis set by systematically increasing the radii to truncate the PT lattice sums starting with a single CH group ($N_c=0$). The opposite character in the distance dependences of $\mathcal{E}^{(3)}$ and $\mathcal{E}_T^{(4)}$ on the one hand, and of $\mathcal{E}_S^{(4)}$ and $\mathcal{E}_{\mathrm{DQ}}^{(4)}$ on the other hand, makes it plausible that the intercellular contributions of these quantities nearly cancel each other and their atomic values dominate the final results.

Within the MBPT scheme, the proper account for electron correlation requires the use of atomic basis functions of high angular momenta that increase (through their nodes) the kinetic energy and thus result in a larger correlation contribution by virtue of the virial theorem. Thinking of electron-electron interactions in terms of the exchange of virtual excitons,[22] these short-range correlation effects are related to quasiparticles with large momentum, i.e., to high-lying conduction bands in the extended BZ. Since, on the other hand, the PT energy denominators associated with these excited states are quite large, it is of interest to see how the balance of these two opposite effects influences our results. Figures 24 and 25 present the various PT terms as functions of the number of conduction bands included in the calculation of the correlation energy. To obtain these figures, exceptionally, the unit cell consisted of two CH units so that there were seven doubly filled valence bands and 35 empty bands in this *t*-PA model. The energy region of the conduction bands was subdivided in steps of approximately one hartree and scattering to virtual excited states was allowed within the number of conduction bands shown in the figures. It is obvious that even the bands with high energy substantially contribute to the different terms and the correlation contribution to ΔE also changes by about 50%.

Turning to the DFT correlation potentials, to get a first impression of their capabilities in describing the above discussed properties of PA, we calculated the equidistant and dimerized geometries of *t*-PA using several combinations of local and gradient-corrected correlation functionals at the DZ basis set level. The corresponding results are shown in Table II. Taking again as measures of quality the experimental value of Δr and the MP4 value of ΔE, we can see that only the exchange-correlation combinations of the type HF-LYP and BHH-LYP lead to acceptable results. Basis set effects and additional structural properties of *t*-PA were calculated, therefore, for these two functionals. The results obtained for r_0, Δr, E_{coh}, and ΔE are depicted in Figs. 14–17 and the corresponding values extrapolated to $N_{\mathrm{CGTO}} \rightarrow \infty$ are collected in Table III.

Figure 22 presents the detailed dependence of E_c on

TABLE III. Energetic and structural parameters of *t*-PA calculated at different theoretical levels as discussed in the text and extrapolated to the limit of a hypothetical infinite atomic basis set. The total energy of the equidistant chain, E(equ), the cohesion energy, E_{coh}(equ), and the energy difference between the alternating and equidistant chains, ΔE, are given in hartree per CH unit, while the optimal C-C distance in the equidistant chain, r_0, the bond alternation, Δr, and the lattice dimerization amplitude, u_0, are given in Å.

Potential	E(equ)	r_0	E_{coh}(equ)	ΔE(alt-equ)	Δr	u_0^a
H	−33.299 247	1.8802	−0.239 946	−0.000 240	0.0986	0.0279
HF	−38.471 820	1.3833	−0.359 888	−0.002 462	0.1196	0.0338
BHH	−38.465 257	1.3883	−0.361 717	−0.001 130	0.1104	0.0312
HFLYP	−38.693 868	1.3588	−0.416 775	−0.001 162	0.1137	0.0321
BHHLYP	−38.697 553	1.3712	−0.420 006	−0.001 202	0.0853	0.0241
MP2	−38.680 974	1.3979	−0.440 952	−0.001 787	0.0786	0.0222
MP4	−38.714 922	1.3975	−0.450 737	−0.001 587	0.0794	0.0224

[a]Experimental value is $u_0 = 0.030$ Å (Ref. 5).

the size of the atomic basis sets for different methods. It is one of the most pleasant properties of the DFT procedures that their correlation energies are nearly independent of the presence of polarization functions. This is not the case for MBPT, which needs very extended basis sets to properly describe correlation effects. Furthermore, the previously obtained MP4 result (−243.1 mhartree correlation energy per CH unit) is in reasonable agreement with the corresponding HF-LYP and BHH-LYP values of −222.05 and −232.3 mhartree, respectively. On the other hand, the local correlation functional VWN with −581 mhartree seriously overestimates E_c. The cohesion energy follows a similar trend: the combination of the LYP functional with the HF and BHH exchanges leads to $E_{coh} = -416.8$ and −420.0 mhartree (Table III), respectively, as compared with the MP2 and MP4 results of −441.0 and −450.7 mhartree, respectively.

Interestingly, the use of the DFT correlation potentials somewhat contracts the *t*-PA lattice (opposite to the PT methods, cf. Figs. 11 and 14) and predicts r_0 values that are by about 0.025–0.030 Å too short in comparison with MP2 and MP4, respectively (Table III). The bond alternation will be, however, reduced using the LYP potential by 0.006 Å for the HF-LYP combination and by 0.025 Å for BHH-LYP. This latter result of 0.0853 Å agrees well with the corresponding MP2 and MP4 values (Table III) and the corresponding dimerization parameter of $u_0 = 0.0241$ Å excellently matches the experiment.[5] The

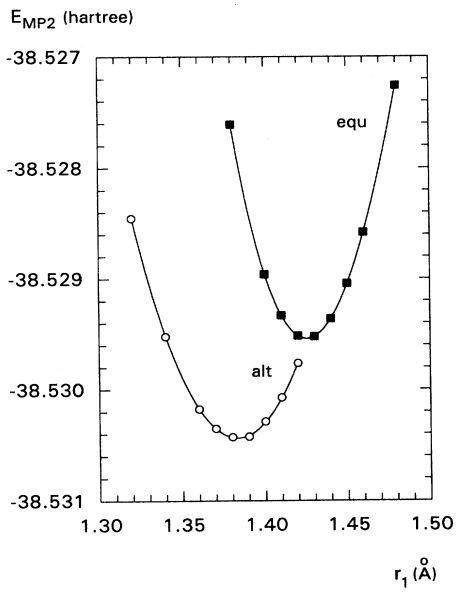

FIG. 18. The MP2 total energy, E_{MP2}, per CH unit of equidistant (equ) and bond-alternating (alt) *t*-PA, as a function of the bond length r_1. For the equidistant chain, the constraint $r_1 = r_2$ has been applied while optimizing all other conformational variables. This constraint was lifted during optimization of the bond-alternating structure.

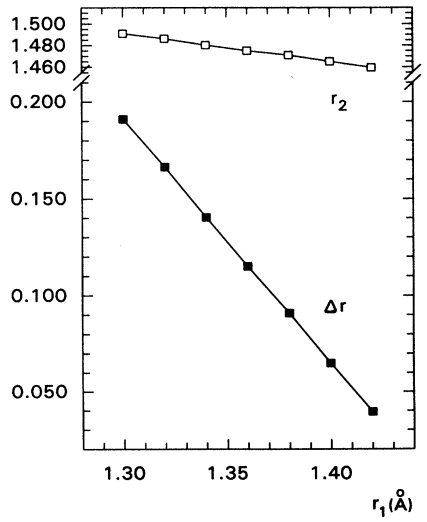

FIG. 19. r_2 and $\Delta r = r_2 - r_1$, as a function of r_1 (defined in Fig. 1) in the case of bond-alternating *t*-PA, obtained for the MP2 method, using the DZ basis set.

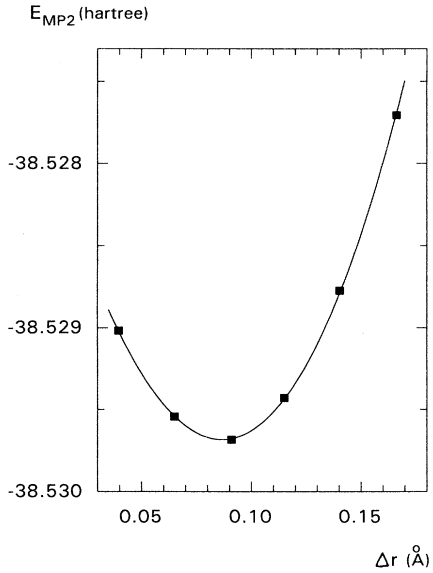

FIG. 20. The MP2 total energy, E_{MP2}, per CH unit of *t*-PA, as a function of the bond alternation, Δr (DZ basis set).

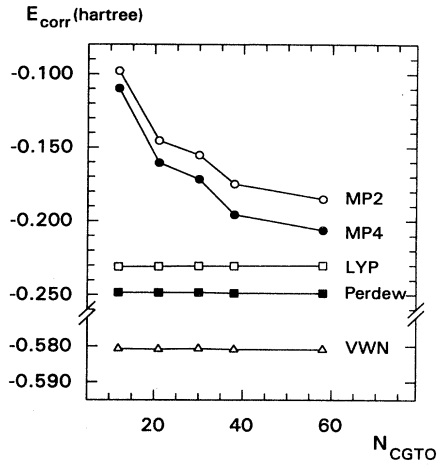

FIG. 22. The correlation energy per CH unit of bond-alternating *t*-PA, as a function of number of CGTO's in the case of different PT and DFT methods.

alternating single and double bond lengths obtained with the BHH-LYP potential are 1.4243 and 1.3390 Å, respectively, providing a lattice constant of $c=2.44$ Å for *t*-PA, again in excellent agreement with the experimental value of 2.46 ± 0.01 Å.[5]

VI. DISCUSSION AND CONCLUSIONS

Density-functional theories certainly belong to the computational methods that have demonstrated their power and capabilities during the past decade, both for atoms and molecules, as well as for simpler solids. It is a promising task, therefore, to investigate their applicability to complex molecular and polymer crystals. One of the primary goals of this paper was, therefore, to study the problem of lattice dimerization in *t*-PA using a couple of exchange-correlation (XC) functionals proposed for molecular applications and compare their performance with the benchmarks provided by high-quality MBPT results on the one hand, and by experimental data on the other one for the same system. Furthermore, to be able to systematically study the physics of the Peierls distortion, we separated the contribution of different potentials to it starting with the pure electrostatic interaction between the atoms in the Hartree approximation. Though

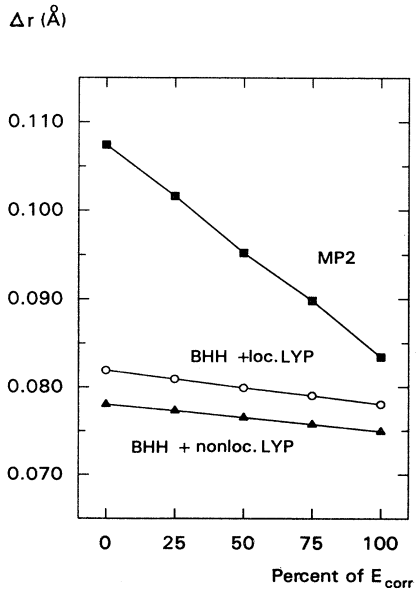

FIG. 21. The bond alternation in *t*-PA, Δr, as a function of different correlation potentials that were turned on stepwise.

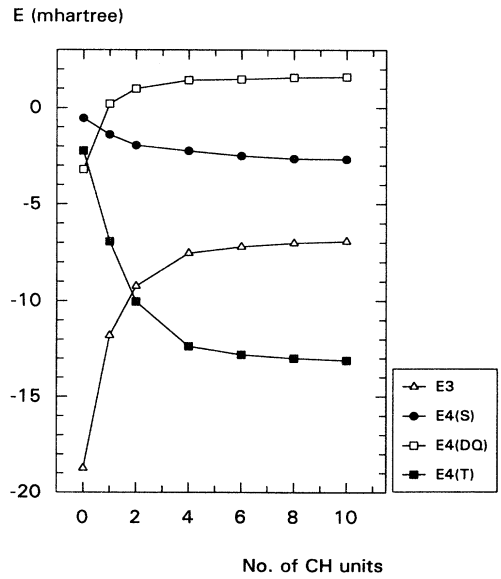

FIG. 23. The dependence of different PT energy terms on the number of CH neighbors that were included in the lattice sums.

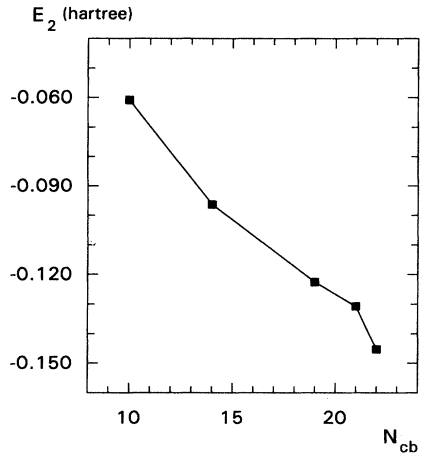

FIG. 24. The dependence of second-order correlation energy per C_2H_2 unit of *t*-PA, on the number of conduction bands included in the calculations.

the resulting Hartree cohesion energy of *t*-PA (−0.24 hartree per CH unit) is only about 60–70% of the values obtained at higher theoretical levels and, consequently, the corresponding C-C bond lengths are by about 30% too long (r_0=1.8802 Å for the equidistant chain), after complete geometry optimization a dimerized Hartree state develops nevertheless with a difference of $\Delta r(H)$=0.0986 Å between the single and double bonds. Scaling down the obtained Hartree bond lengths from about 1.9 Å to the chemically reasonable value of 1.4 Å, this bond alternation would correspond to about Δr=0.06−0.07 Å. The extra Hartree binding energy due to dimerization (−0.24 mhartree per CH unit) is, of

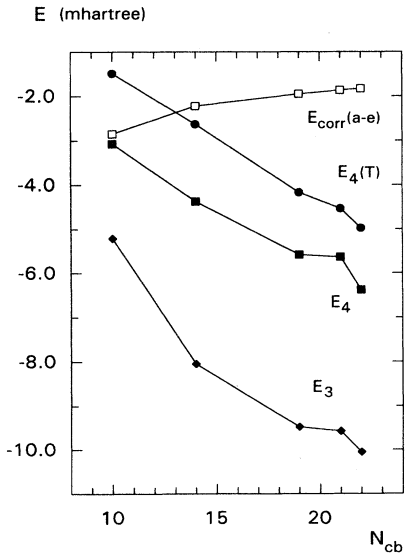

FIG. 25. The dependence of various third- and fourth-order terms, for the C_2H_2 unit of *t*-PA, on the number of conduction bands included in the calculations.

course, rather small but definitely significant with respect to the accuracy of our calculations.

Upon turning on the exact (HF) exchange potential, the cohesion energy of *t*-PA decreases to −0.36 hartree per CH unit, the C-C bond length of the equidistant chain is reduced to r_0(HF) = 1.3833 Å, and the bond alternation increases to Δr(HF) = 0.1196 Å corresponding to u_0=0.034 Å. The dimerization energy of the estimated HF limit, obtained by extrapolation to a hypothetical infinite atomic basis set, is ΔE(HF) = −2.46 mhartree (−0.067 eV) per CH unit. Electron correlation somewhat expands the equidistant lattice at both the MP2 and MP4 levels (to r_0=1.3979 and 1.3975 Å) and reduces the bond alternation (to Δr=0.0786 and 0.0794 Å, respectively). These values correspond to a dimerization parameter of u_0=0.022 Å, which is close to the experimental value of 0.026 A.[5] The predicted lattice constant of c=2.48 Å also reproduces the experimental one (2.46±0.01 Å). The absolute value of the correlation energy is −209.2 mhartree (−5.69 eV) per CH at MP2 and −243.1 mhartree (−6.62 eV) at MP4. Electron correlation also provides a significant contribution to the cohesion energy of *t*-PA (−81.1 and −90.8 mhartree), leading to E_{coh}(MP2) = −0.441 hartree and E_{coh}(MP4) = −0.451 hartree, respectively.

Regarding the above quantities as benchmarks, it turns out that the DFT procedures using Slater exchange (with or without additional correlation potentials) all seriously underestimate the bond alternation effect, both from the geometrical and energetical points of view, leading to u_0=0.002–0.008 Å and ΔE=−0.1–−0.2 mhartree (Table II), in agreement with previous investigations using similar functionals.[46–48] Gradient corrections have proved to be very important both for E_x and E_c. From the DFT exchange potentials, the hybrid functional BHH mixing the exact and the Slater exchange seems to be the most successful. When combined with the gradient-corrected correlation functional LYP, it not only properly describes cohesion (with E_c=−0.420 hartree), but also leads to the very reasonable value of Δr =0.0853 Å (u_0=0.024 Å) and to the dimer stabilization energy of ΔE=−1.2 mhartree, comparable with the MBPT values above. The BHH-LYP method is definitely better than the simple HF-LYP, which tends to overestimate Δr leading to u_0=0.032 Å.

In previous papers,[22,27] we also reported the band structures and forbidden gaps of *t*-PA, both for the HF theory and for MBPT, using the quasiparticle (electron polaron) picture to correct the valence and conduction bands, respectively, for correlation effects. Since the Kohn-Sham eigenvalues of the DFT description do not have a physical meaning themselves,[39–43] which would relate them to the HF or to the quasiparticle band structures, it would not be a fair attempt to compare the DFT band structures of *t*-PA obtained in this work either with the previous results or with experiments. Instead, we are going to use them as an input to compute the band gap of PA within the framework of the GW method[68,69] that provides a physically more meaningful basis to compute band structures for DFT. The corresponding results will

appear in a forthcoming paper.[70]

In summary, our results show that the exchange potentials derived from the homogeneous electron gas model are not capable of realistically describing the Peierls-type dimerization in *t*-PA. Gradient corrections for the exchange and correlation terms are needed as well to improve the theory. After introducing such corrections, however, the BHH-LYP functional proved to be equivalent to the computationally much more demanding MBPT methods in predicting the structural and energetical properties of this polymer crystal. These experiences encourage us to extend these investigations in the near future to other solids of this kind, as well as to treat impurity effects, vibrational, dielectric, and transport properties of polymers within the same theoretical framework.

ACKNOWLEDGMENTS

The author is indebted to J. W. Mintmire for the use of his $X\alpha$ polymer program in an early phase of this work, to M. Seel for the implementation of the multipole expansion technique, and to B. Hübner, S. Attinger, J. Keese, and B. Scholz for contributing to the MP3 and MP4 modules of the POLYGAUSS program system. The generous support with computer time on the CONVEX and CRAY supercomputers and on IBM/SP2 and SGI Power Challenge clusters of DKFZ and of the University of Stuttgart are also gratefully acknowledged. This research has been partly supported by the Commission of the European Union (Grant No. CT-93-006) and by the German Federal Ministry of Research and Technology (Grant No. 01 1B 303A).

[1]D. Baeriswyl, D. K. Campbell, and S. Mazumdar, in *Conjugated Conducting Polymers,* edited by H. G. Kiess (Springer-Verlag, Berlin, 1992).
[2]J. Paldus and P. Piecuch, Int. J. Quantum Chem. **42**, 135 (1992).
[3]W. Förner, Adv. Quantum Chem. **25**, 207 (1994).
[4]J. Tsukamoto, Adv. Phys. **41**, 509 (1992).
[5]C. R. Fincher, Jr., C.-E. Chen, A. J. Heeger, A. G. macDiarmid, and J. B. Hastings, Phys. Rev. Lett. **48**, 100 (1982).
[6]H. Kahlert, O. Leitner, and G. Leising, Synth. Met. **17**, 467 (1987).
[7]P. E. Sokol, G. Tai, C. Gordon, A. J. Epstein, R. Weagly, and J. D. Jorgensen, Bull. Am. Phys. Soc. **31**, 330 (1986).
[8]C. S. Yanoni and T. C. Clark, Phys. Rev. Lett. **51**, 1191 (1983).
[9]R. Peierls, *Quantum Theory of Solids* (Clarendon, Oxford, 1955), p. 108.
[10]D. J. Thouless, *The Quantum Mechanics of Many-body Systems* (Academic, New York, 1961).
[11]J. Cizek and J. Paldus, J. Chem. Phys. **47**, 3976 (1967).
[12]H. Fukutome, Prog. Theor. Phys. **40**, 998, 1227 (1968).
[13]J.-L. Calais, Int. J. Quantum Chem. **11S**, 547 (1977).
[14]J. W. Mintmire and C. T. White, Phys. Rev. B **35**, 4180 (1987).
[15]P. Vogl and D. K. Campbell, Phys. Rev. Lett. **62**, 2012 (1989).
[16]P. Vogl and D. K. Campbell, Phys. Rev. B **41**, 12 797 (1990).
[17]J. Ashkenazi, W. E. Pickett, H. Krakauer, C. S. Wang, B. M. Klein, and S. R. Chubb, Phys. Rev. Lett. **62**, 2016 (1989).
[18]M. Springborg, J.-L. Calais, O. Goscinski, and L. A. Erikson, Phys. Rev. B **44**, 12 713 (1991).
[19]J. Paloheimo and J. von Boehm, Phys. Rev. B **46**, 4304 (1992).
[20]J. Paloheimo and J. von Boehm, Synth. Met. **55-57**, 4443 (1993).
[21]J. P. Perdew and A. Zunger, Phys. Rev. B **2**, 5048 (1981).
[22]S. Suhai, Phys. Rev. B **27**, 3506 (1983).
[23]S. Suhai, Chem. Phys. Lett. **96**, 619 (1983).
[24]S. Suhai, Phys. Rev. B **29**, 4570 (1984).
[25]G. König and G. Stollhoff, Phys. Rev. Lett. **65**, 1239 (1990).
[26]S. Suhai, J. Chem. Phys. **84**, 5071 (1986).
[27]S. Suhai, Int. J. Quantum Chem. **42**, 193 (1992).
[28]S. Suhai, Int. J. Quantum Chem. **QCS-27**, 131 (1993).
[29]S. Suhai, J. Chem. Phys. **101**, 9766 (1994).
[30]S. Suhai, Phys. Rev. B **50**, 14 791 (1994).
[31]J. A. Pople, J. S. Binkley, and R. Seeger, Int. J. Quantum Chem. Symp. **10**, 1 (1976).
[32]R. Krishnan and J. A. Pople, Int. J. Quantum Chem. **14**, 91 (1978).
[33]R. Krishnan, J. A. Pople, E. S. Reploge, and M. Head-Gordon, J. Phys. Chem. **94**, 5579 (1990).
[34]M. J. Frisch, G. W. Trucks, M. Head-Gordon, P. M. W. Gill, M. W. Gong, J. B. Foresman, B. G. Johnson, H. B. Schlegel, M. A. Robb, E. S. Replogle, R. Gomperts, J. L. Andres, K. Raghavachari, J. S. Binkley, C. Gonzalez, R. L. Martin, D. J. Fox, D. J. Defrees, J. Baker, J. J. P. Stewart, and J. A. Pople, Computer Code GAUSSIAN92, Gaussian, Inc., Pittsburgh, PA, 1992.
[35]P. M. W. Gill, B. G. Johnson, and A. J. Pople, Int. J. Quantum Chem. Symp. **26**, 319 (1992).
[36]P. M. W. Gill, B. G. Johnson, and A. J. Pople, Chem. Phys. Lett. **197**, 499 (1992).
[37]B. G. Johnson, P. M. W. Gill, and J. A. Pople, J. Chem. Phys **98**, 5612 (1993).
[38]P. Hohenberg and W. Kohn, Phys. Rev. B **136**, 864 (1964).
[39]W. Kohn and L. J. Sham, Phys. Rev. A **140**, 1133 (1965).
[40]G. Senatore and N. H. March, Rev. Mod. Phys. **66**, 445 (1994).
[41]E. S. Kryachko and E. V. Ludena, *Energy Density Functional Theory of Many-Electron Systems* (Kluwer, Dordrecht, 1990).
[42]*Advances in Quantum Chemistry,* edited by S. B. Trickey (Academic, New York, 1990), Vol. 21.
[43]R. G. Parr and W. Yang, *Density-Functional Theory of Atoms and Molecules* (Oxford University Press, New York, 1989).
[44]*Density Functional Methods in Chemistry,* edited by J. K. Labanowski and J. Andzelm (Springer, New York, 1991).
[45]T. Ziegler, Chem. Rev. **91**, 651 (1991).
[46]J. W. Mintmire and C. T. White, Phys. Rev. Lett. **50**, 101 (1983).
[47]J. W. Mintmire and C. T. White, Phys. Rev. B **27**, 1447 (1983).
[48]J. von Boehm, P. Kuivalainen, and J.-L. Calais, Phys. Rev. B **35**, 8177 (1987).
[49]M. Springborn and O. K. Andersen, J. Chem. Phys. **87**, 7125 (1987).
[50]G. te Velde and E. J. Baerends, Phys. Rev. B **44**, 7888 (1991).
[51]G. Del Re, J. Ladik, and G. Biczó, Phys. Rev. **155**, 967 (1967).
[52]J. M. André, L. Gouverneur, and G. Leroy, Int. J. Quantum Chem. **1**, 427 (1967).
[53]S. Suhai, in Molecules in *Physics, Chemistry, and Biology,* edited by J. Maruani (Kluwer, Dordrecht, 1989), Vol. IV, pp. 133–194.
[54]C. Moeller and M. S. Plesset, Phys. Rev. **46**, 618 (1934).

[55]J. C. Slater, *Quantum Theory of Molecules and Solids* (McGraw-Hill, New York, 1974), Vol. 4.
[56]R. Colle and O. Salvetti, Theor. Chim. Acta **37**, 329 (1975).
[57]S. H. Vosko, L. Wilk, and M. Nusair, Can. J. Phys. **58**, 1200 (1980).
[58]J. P. Perdew, Phys. Rev. B **33**, 8822 (1983).
[59]J. P. Perdew and Y. Wang, Phys. Rev. B **33**, 8800 (1986).
[60]A. D. Becke, Phys. Rev. A **38**, 3098 (1988).
[61]C. Lee, W. Yang, and R. G. Parr, Phys. Rev. B **37**, 785 (1988).
[62]B. Mielich, A. Savin, H. Stoll, and H. Preuss, Chem. Phys. Lett. **157**, 200 (1989).
[63]A. D. Becke, J. Chem. Phys. **98**, 5648 (1993).
[64]G. Raether and S. Suhai, J. Chem. Phys. (to be published).
[65]T. H. Dunning and P. J. Hay, *Modern Theoretical Chemistry* (Plenum, New York, 1976), p. 1.
[66]T. H. Dunning, J. Chem. Phys. **55**, 716 (1971).
[67]T. H. Dunning, J. Chem. Phys. **90**, 1007 (1989).
[68]M. Schlüter and L. J. Sham, Adv. Quantum Chem. **21**, 97 (1990).
[69]M. S. Hybertsen and S. G. Louis, Adv. Quantum Chem. **21**, 155 (1990).
[70]S. Suhai (unpublished).